International Journal of Scientific Research Engineering & Technology (IJSRET)
Volume 1 Issue5 pp 184-189 August 2012 www.ijsret.org ISSN 2278 – 0882

Optical Fibre Communication: Optimiztion Using Simulation

Pallavi Gupta[1] , Rahul Sharma[2], Manoj Kumar Chauhan[3], Lavi Agarwal[4]
[1-4]EN Department, [1-4]IIMT IET, Meerut
[1]guptapallavi864@gmail.com
[2]er.rahul2007@gmail.com
[3]Manojchauhan.mit@gmail.com
[4]lavigarg07@gmail.com

ABSTRACT
The existing wireless systems can hardly provide transmission capacity of the order of few Mbps. However, wireless optical fiber technology has the potential of providing data capacity of the order of Mbit/sec and Tbit/sec, respectively. Therefore the requirements of optical broadband wireless system can be met through the integration of optical communication fiber and millimeter wave optical wireless systems. Terrestrial optical wireless communication network is emerging as a promising technology, which makes connectivity possible between high rise buildings and metropolitan and intercity communication infrastructure this paper presents simulated and measured microwave properties of InP-InGaAsP TWEAM. Obtaining the experimental results included design, process, and characterization of the TWEAM structures for the application of optical fiber communication .A measured TWEAM modulation response is also presented in the paper and agrees very well with the circuit model simulation using the experimentally found microwave properties. This agreement allows the extrapolation of the response to frequencies beyond the characterization limit (45GHz) of the used setup. This paper present Device design, process design, full-wave simulations, processing, results of a new high-impedance design in form of a segmented TWEAM. The devices were processed within the frame of this work and record bandwidth performance is reported. At 50- impedance a bandwidth in the 90GHz region was indicated.

Keywords: *optical fiber communication, long distance wireless system, optical waveguide, Microwave properties, circuit model analysis*

I. INTRODUCTION
Optical wireless communication network is gaining acceptance in an increasing number of sectors of science and industry, owing to its unique combination of features: Extremely high bandwidth, rapid deployment time, license and tariff-free bandwidth allocation, and low power consumption, weight, and size. The demand of high signal bandwidth and high bit rate in optical wireless communications is growing exponentially day by day, as the numbers of users have been increased drastically. The next generation wireless communication systems therefore need to be of higher standards, so as to support various broadband wireless services such as, video conferencing, videophones, high-speed internet access, etc. External modulators will become key components in fiber optical communication systems operating at 40Gbit/s and higher bitrates. Semiconductor electro-absorption (EA) modulators are promising candidates because of their high-speed potential, and their process compatibility with the corresponding semi-conductor laser light sources. The traveling-wave (TW) electrode concept for electro optic modulators has been used for a long time in order to resolve the conflict between high modulation depth and high modulation bandwidth. Recently, it has been adopted for EA modulators as well. The starting worked platform is external modulator microwave design and FEM full-wave simulations. The experimental results are then compared to these simulations from the experimental data circuit model parameters are extracted and used to simulate the modulation response of a corresponding TWEAM.

II. PRINCIPLE OF FIBER-OPTIC COMMUNICATION SYSTEMS
The simplest model of a light wave system consists of a transmitter, a transmission medium such as an optical fiber, and a detector (see Figure 1.2). Information to be transmitted is digitized into 1's or 0's (also referred to as bits) and an optical pulse representing this information is then sending using a laser and a modulator. Semiconductor lasers are capable of emitting sufficient powers (10 mW) and have a relatively high coupling efficiency (50% into single mode fiber). Consequently, semiconductor lasers are the sources of choice for long-haul communication systems. There are currently two formats for encoding optical bit streams, nonreturn-to-zero(NRZ) and return-to-zero (RZ) .An optical pulse representing RZ encoding is

shorter than NRZ pulse, and its amplitude returns to zero before the bit duration is over. For a NRZ pulse, the amplitude of a "1" does not return to zero during the bit duration; therefore, two successive 1s are merged into a pulse that is twice as long. Currently, the NRZ format is predominately used because of its intrinsically smaller signal bandwidth; however, for systems based on soliton principles, the RZ format must be used.

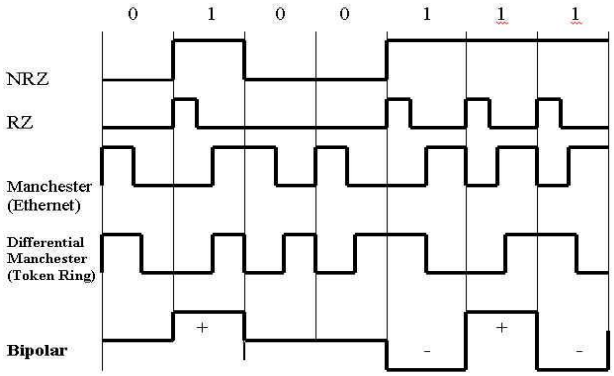

Figure 1

The optical bit stream is transported through optical fibers from one location to another. The capacity of a fiber-optic communication system is designated by the number of bits it can send per second, or alternatively, by the inverse of the bit slot. Thus a system transmitting 100-ps pulses using NRZ or 25-ps pulses using RZ (with pulse separation equal to four times the pulse width) will carry a single channel capacity of 10 Gb/s. The receiver's role is to convert the optical signal received from the optical fiber back to the original electrical signal. Modern systems use the direct-detection scheme, which typically consists of a semiconductor detector, a clock-recovery circuit, and a decision-making circuit to identify bits as 1 or 0. The performance of fiber-optic communication systems is characterized by the number of errors made per second accounted by its receiver circuit, or the bit-error rate (BER). Typically, a system is specified as having error-free transmission when it has BER of less than 10−9. With novel coding algorithms, systems can gain several dB in performance using forward error correction (FEC).

III. LONG DISTANCE COMMUNICATION

An outdoor long distance optical wireless system consists of three parts: transmitter, propagation path and receiver. In order to accommodate the high-speed operation (e.g. multi Gbit/sec or higher), the transmitter usually utilizes semiconductor lasers with broad bandwidth and high launch power. The receiver employs a trans-impedance design, which makes a good compromise between band-width and noise, combined with bootstrapping that reduces the effective capacitance of the photodiode. Typical (bootstrapping) receivers use either (optically pre-amplified) PIN or avalanche photodiodes (APD) of different dimensions. The power budget and raw-data performance of an optical wireless link are subject to atmospheric loss along the propagation path, which includes free space loss, clear air absorption, scattering, refraction and atmospheric turbulence (or scintillation). Free space loss defines the proportion of optical power arriving at the receiver that is effectively captured within the receiver's aperture and exists in all indoor and outdoor systems. Other forms of channel impairment are experienced only by outdoor systems. Air absorption, scattering and refraction are closely related to weather (for example, fog, mist and snow). Nevertheless, field tests conducted in major cities around the world show that the atmospheric attenuation due to these factors is consistently low.

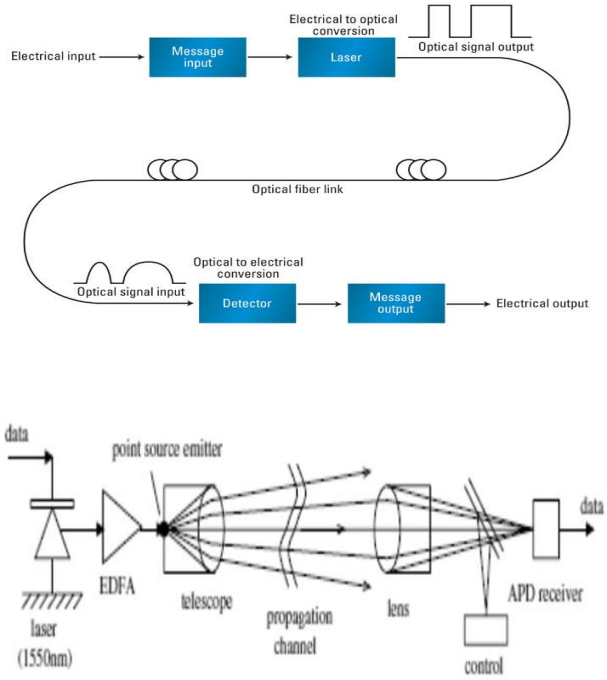

Figure 2

IV. THE OPTICAL WAVEGUIDE

The optical waveguide used the intrinsic cross-sectional geometry of the TW-EAM. The waveguide core region is the absorption region of the modulator, which from the electrical point of view presents the depletion layer of a double-hetero pin-structure. Therefore, electrical, optical, and electro-optical designs are interlocked. The thickness

of the core region determines the electric field strength for a given applied voltage. The value of the dependent absorption coefficient in-side this material is subject to its band gap compared to the photon energy. The effective waveguide index denotes the optical velocity, which is a parameter in the high frequency TWEAM design. Further important for the extinction ratio of the EA modulator is, apart from its length, the transverse mode confinement. Only the fraction of the optical mode confined within the modulation region will be modulated. This modal electro-absorption is thus the equivalent to the transverse modal gain as defined for semiconductor lasers .Another important parameter is the zero-bias optical propagation loss, which is a function of the band gap, the quality of the waveguide, and the doping levels of the surrounding semiconductor layers. The main material parameters that are needed in order to perform waveguide simulations are the refractive indices. Material data gained from experiments can be found.

Source	T	material	x	y	E_g	refractive index n
Adachi [82, 83]	room	InP	0	0	1.35eV	3.17
		Q(1.48)	0.359	0.773	0.838eV	3.41
Weber [75]	295K	InP	0	0	1.35eV	3.18
		Q(1.48)	0.385	0.827	0.838eV	3.51

Fig 3: Refractive index of InP/In1¡xGaxAsyP1¡y (lattice matched), for photon energies of 0.8eV (¸=1.55¹m)

The waveguide simulations have to consider 2-dimensional structures with non-uniform refractive index in each direction. Approximate solutions, such as provided by the effective index technique may be used. Otherwise, numerical simulation tools are necessary. The simulated curves shown in this section are obtained with the help of commercial software for the simulation of 2-and 3-dimensional optical waveguide structures using a rigorous fully vectorial formalism A waveguide mesa of the width wm is etched through the vertical pin InP/InGaAsP/InP structure. The mesa is planarized using either polymer based low refractive index dielectric, like BCB (n=1.64), or by regrowing semi-insulating InP (n=3.18). The mesa etching stops right after the waveguide core layer forming the so-called ridge-waveguide structure. The resulting lower mesa is also planarized using BCB. All cases are considered for an optical wavelength of 1.55¹m.

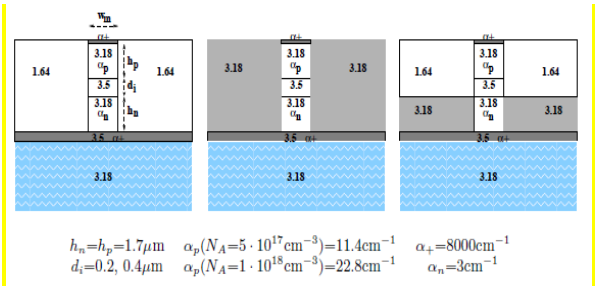

Figure 4

The mode loss characteristics are drawn in fig. In these simulations the mode loss is exclusively caused by free carrier absorption in the doped semiconductor layers. In particular, p-doped InP is a very lossy material. Two typical doping levels have been assumed for the simulations (5.10^{17}, $10^{18}cm^{-3}$). The corresponding loss parameters are obtained from For d_i=0.4µ meter the structures do not show any significant differences. For diameter 0.2 micro meter the loss starts to increase dramatically for the ridge waveguide structure since the mode gets coupled to the lower highly absorbing (α_+) InGaAs contact layer. For real structures either h_n should be increased or the InGaAs layer omitted, which is usually done in practice. It has to be remarked that the simulations do not include any loss caused by side wall etch damage. Regarding this loss factor, the ridge structure is expected to be superior because of the shorter etch distance. The impact of very lossy materials, like contact layers and metals, on the mode propagation can be severe if certain safety distances are not adjusted within the structure (compare discussion above). Figure h_p=1.7micro m was chosen as the p-layer thickness. Coming too close to the highly absorbing InGaAs-layer (which has usually also a metal on top) would destroy the optical mode. Furthermore, a low p-doping would be desirable for low optical loss. These requirements on p-layer thickness and doping are unfortunately exactly inverse for the high-frequency design. Therefore, nothing better than a compromise can be found here. The effective mode index denotes the optical speed, which should be known in the design of a traveling-wave modulator. However, for TWEAM design the precise knowledge of this value is not of very high importance since these modulators are very short and lossy as compared to electro-optic TW phase modulators. Nevertheless, an approximate number should be known in order to use it as a parameter in the modeling of the modulation response . For all simulations with a core layer thickness of di=0.2µm, n_{opt} is in the range of 3.2. . . 3.25 and 3.27. . . 3.33 for d_i=0.4µm.

International Journal of Scientific Research Engineering & Technology (IJSRET)
Volume 1 Issue5 pp 184-189 August 2012 www.ijsret.org ISSN 2278 – 0882

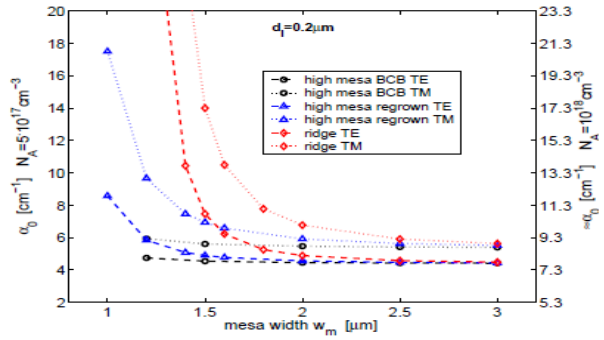

Fig 5: Mode loss α_0 as a function of mesa width for different core layer thicknesses and p-doping levels.

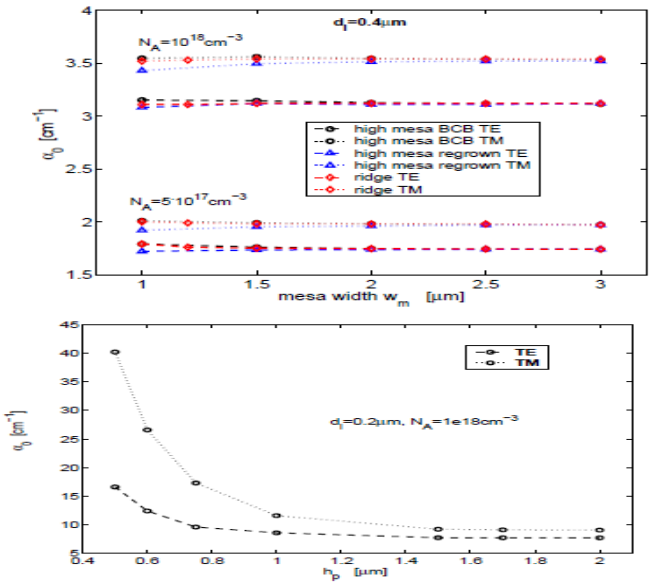

Fig 6: Optical loss as a function of separation from the highly lossy electrical contact layer (high mesa BCB structure).

V. THE CIRCUIT MODEL

A very useful way to analyze the TWEAM is with the help of an equivalent circuit model. The use of such a model is based on the assumption of quasi-TEM waves propagating along the electrical waveguide, i.e., the lossy modulator transmission line (TML).Unique voltage and current waves can be associated with the electro-magnetic field solution of the TEM wave .Provided that the circuit model elements are known, the modulating volt-age can directly be obtained, which allows the calculation of the modulation frequency response. However, in order to find the values of the circuit model elements wave solutions or experimental data are required

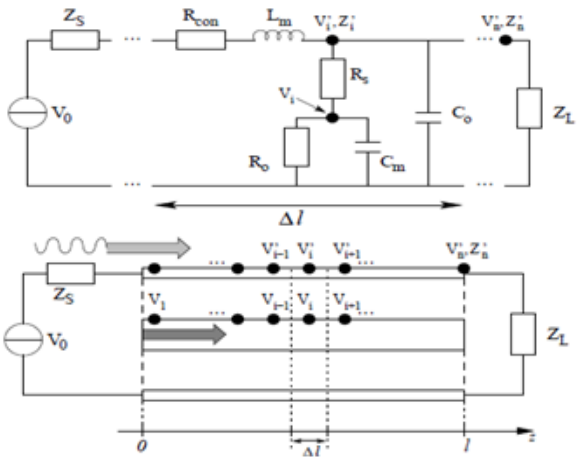

Figure The TWEAM circuit model. R_{con}, L_m, $\frac{1}{R_s}$, $\frac{1}{R_o}$, C_m, C_o are defined per unit length.

Figure 7

VI. MICROWAVE PROPERTIES AND CIRCUIT MODEL ANALYSIS

With the knowledge of the microwave properties characteristic impedance Zc and propagation constant γ of the TWEAM-TML, and with the assumption of an appropriate circuit model, the small signal modulation response can be calculated.

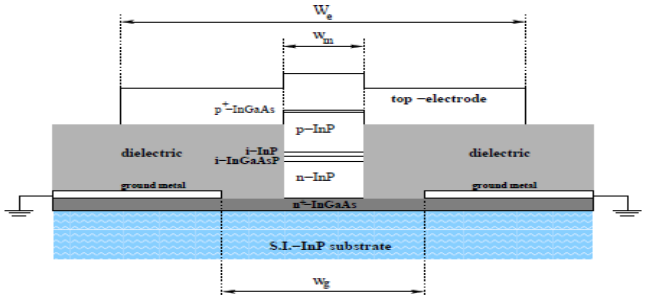

layer	thickness [μm]		σ [(Ωm)⁻¹]		ϵ_r
top-electrode	t_{top}	2.5	$4.54 \cdot 10^7$		
p^+-InGaAs	t_{p+}	0.1	$1.80 \cdot 10^3$		14.1
p-InP	h_p	1.5	$1.52 \cdot 10^3$	($N_A = 10^{18}$cm^{-3})	12.4
i-InP	d_t	0.2	0		12.4
i-InGaAsP		0.2	0		14.0
n-InP	h_n	1.7	$3.70 \cdot 10^4$	($N_D = 10^{18}$cm^{-3})	12.4
n^+-InGaAs	t_{n+}	0.6	$5.00 \cdot 10^4$		14.1
ground metal	t_g	0.3	$4.54 \cdot 10^7$		
substrate			0		12.4
dielectric (BCB)	$(h_n+d_t+h_p+t_{p+})$-0.5		0		2.7

Fig 8: Simulated structure and material parameters.

Carrier Concentration cm^{-3}	ρ Ωcm	σ $(\Omega cm)^{-1}$	R_p $(h_p = 1.5\mu m)$ Ωmm	
			$w_m = 1\mu m$	$w_m = 2.4\mu m$
$1 \cdot 10^{15}$	42	0.024	630	262.5
$1 \cdot 10^{16}$	4.5	0.222	67.5	28.125
$1 \cdot 10^{17}$	0.48	2.083	7.2	3.0
$1 \cdot 10^{18}$	0.066	15.15	0.99	0.4125
$7 \cdot 10^{18}$	0.020	50.0	0.3	0.125

Fig 9: Resistivity of p-type InP [99] (300K) and the resulting p-layer resistance

VII. RESULTS AND DISCUSSION

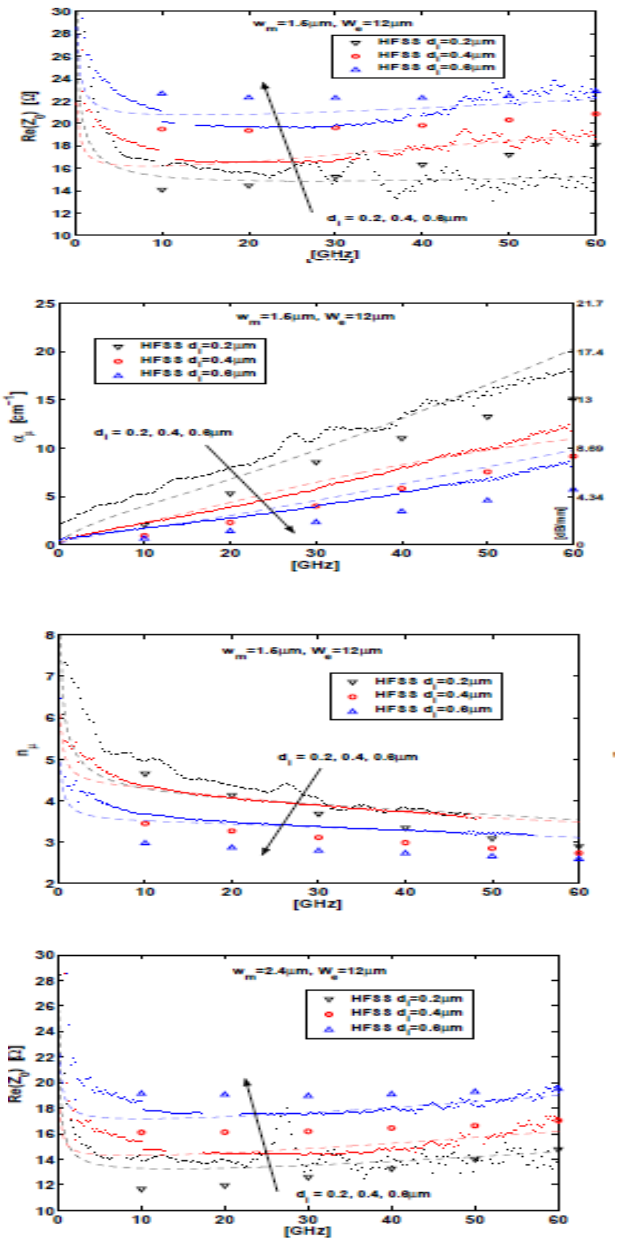

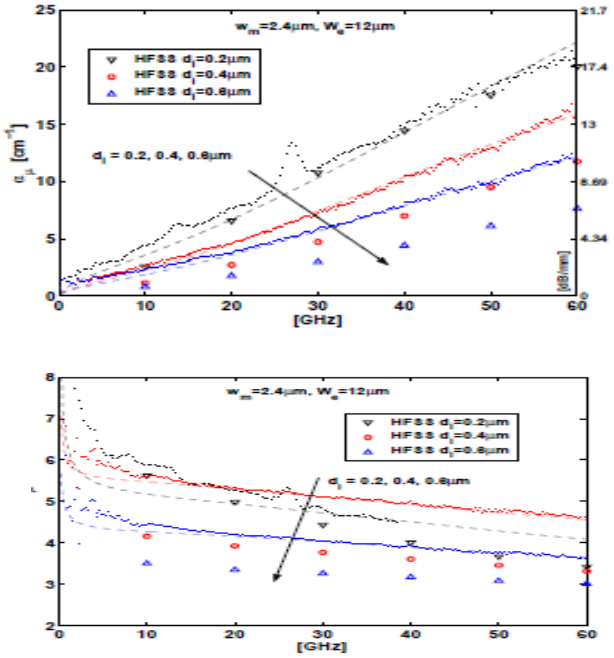

Fig 10: Impedance, microwave index, and microwave attenuation for different depletion layer thicknesses, and for mesa widths of 1.5µm (left hand side) and 2.4µm (right hand side), respectively. The dotted lines represent the experimental values. Dashed lines are circuit model fits.

VIII. RESULT & CONCLUSION

In this paper we have discussing various mode and simulation to improving the capability of optical wireless network and shows the results obtained from measurements on three different epitaxial structures. The intrinsic layer thickness di has been varied. The depletion layer of the first structure (di=0.2µm) is the Q(1.48). InGaAsP layer. For the second structure a 0.2µm-i-InP buffer layer is added on top of the InGaAsP material. The third structure is grown with an additional un-doped InP-buffer layer under neath the Q-material resulting in di=0.6µm.The three structures were characterized for mesa widths of 1.5¹m and 2.4µm, respectively. In these measurements are compared to HFSS simulations. The p-doping is 10^{17} cm^{-3} , and h_p/h_n of the three structures are 1.7/1.7, 1.5/1.7, and 1.5/1.5µm, respectively. The other parameters are as specified in fig. As expected, a thicker intrinsic layer results in higher impedance, lower propagation loss, and lower microwave index. All these three effects can be attributed to a reduction in capacitance per unit length. A narrower mesa produces the same effect. However, a narrower mesa does also result in a reduced vertical conductance per unit length (i.e., higher Rs), which leads to an increase of α_μ. Still, for

the configurations compared here, the 1.5μm wide mesa exhibits lower electrical loss than the 2.4μm wide mesa, which is confirmed by both simulations and measurements. The Simulations and experiment agree very well in that they show the same tendency when changing structure parameters and frequency. The impedance values show the best agreement. The simulated α_{μ} values systematically under estimate the loss that is eventually obtained from measurements on real structures. This is not too surprising since the actual gold conductivity might be lower than the theoretical value. Furthermore, rough mesa edges and conductor surfaces are not considered in the simulation.

REFERENCES

[1] I. Akyildiz, ”A survey on wireless mesh networks”, IEEE Radio Commun. Vol. 43, No. 9, Sep. 2005, pp.S23-S30.

[2] Chang-Hee Lee, Wayne V. Sorin, ”Fiber to the Home Using a PON infrastructure”, Journal of light wave technology, Vol. 24, No. 12, Dec. 2006, pp. 4568-4583.

[3] S. Sakar et al., ”Hybrid Wireless-Optical Broadband-Access Network(WOBAN): A Review of Relevant Challenges”, Journal of Light wave Technology, Vol.25, No.11, Nov. 2007, pp. 3329-3340

[4] S. Sarkar et al, ”A Mixed Integer Programming Model for Optimum Placement of Base Stations and Optical Network Units in a Hybrid Wireless-Optical Broadband Access Network (WOBAN)”, IEEE WCNC 2007, pp. 3907-3911

[5] S. Sarkar et al., ”Towards global optimization of multiple ONUs placement in hybrid optical-wireless broadband access networks”, in Proc. COIN, Jul. 2006, pp.65-67.

[6] Saurabh Bhandari, ”Hybrid Optical Wireless Networks”,ICNICONSM 2006.

[7] S. Sarkar, H. Yen, S. Dixit, and B. Mukherjee, ”DARA: Delay aware routing algorithm in a hybrid wireless-optical broadband access network (WOBAN)”, in Proc. IEEE ICC, Jun. 2007, pp.2480-2484.